

Study on Ash Characteristics of Cofiring Sawdust with Coal for supercritical power plants in Indonesia

Hariana¹, Fairuz Milkiy Kuswa¹, Muhammad Huda², Arif Darmawan^{1*}

1 The National Research and Innovation Agency (BRIN), Indonesia.

2 The Center of Certification Indonesian State Electric Company (PT PLN) Jakarta Selatan, Indonesia.

ABSTRACT

Currently, Low-rank coal and medium-rank coal dominate Indonesian coal. Unfortunately, although Indonesia produces coal, the coal reserve is relatively limited. On the other hand, the use of biomass has many obstacles and has low thermal efficiency. Cofiring biomass and coal is believed to be an excellent solution to answering these problems and extending the life of power plants. This paper presents experimental investigations into the cofiring of sawdust with pulverized coal using a drop tube furnace. The ash particles characteristic and material composition were also analyzed using scanning electron microscopy with energy dispersive X-ray (SEM-EDX). The results indicate that cofiring sawdust with coal during combustion impact ash characteristics due to fuels' varied physical and chemical properties. The slagging issue is still safe in follow-up observations from prior research involving the addition of 10% sawdust biomass to cofiring in pulverized coal supercritical boilers using a combination of DTF and SEM methodology. Substituting 10% of biomass for coal could have a big impact on supercritical power plants in Indonesia, with a capacity of 5-6 GW

Keywords: cofiring, biomass, sawdust, drop tube furnace, SEM-EDX, ash.

1. INTRODUCTION

Indonesia has the advantage of being a tropical country with many energy variations, such as biomass as an alternative fuel blending in the future [1]. Various types of biomass can be used, ranging from agriculture, forestry, and plantations [2]. In everyday use, these

technologies can be used together to complement each other in a single process so that the final product with higher efficiency is produced, as happened in the solid biomass process [3][4]. Biomass fuel can be used as a mixed or independent fuel in power generation, with a stable output capacity. The solid fuels commonly used are biomass, municipal solid waste [5], agricultural waste [6], and wood and timber industry waste [7]. Sawdust is one of the biomass potentials as a fuel alternative. Indonesia has a large raw material for wood and is listed as one of the largest exporting countries in the world.

Ash content in biomass, one of the largest components in causing combustion problems, varies widely and tends to be low. In wood instead of sawdust, the amount of ash is 2 percent, while in agricultural waste, the amount of ash reaches 5%–10%, and the largest is in rice husks (rice husk) 30%–40%. In low-calorie coal, the ash content reaches 40% [8]. The high ash content in sawdust can cause slag on the surface of the pipes in the boiler, causing a decrease in the heat transfer ability in the furnace [9]. In addition, another impact of high ash content is that it can reduce combustion stability. The most dominant alkali content is in the biomass ash, such as Na (sodium) and K (potassium) [10]. Potassium has an impact on corrosion, while sodium to emissions, namely the formation of aerosols. These two elements also have an impact on decreasing the ash fusion temperature [11].

This paper presents experimental investigations into the cofiring of sawdust with pulverized coal using a drop tube furnace. The ash particles characteristic and material composition were also analyzed deeply using scanning electron microscopy with energy dispersive X-ray (SEM-EDX).

Selection and peer-review under responsibility of the scientific committee of the 13th Int. Conf. on Applied Energy (ICAE2021).

Copyright © 2021 ICAE

2. EXPERIMENTAL METHODS

2.1 Samples preparation

Before being cofired, the coal and sawdust samples were obtained and reduced in size to study its characterization, including their ash elemental analysis. The sawdust and coal mixture for the DTF parameter is 10% sawdust and 90% coal with 200 mesh samples. In addition, table 1 shows the ash elemental analysis of the combination of sawdust and coal.

2.2 Combustion chamber and ash analyses

Coal and sawdust samples were tested for combustion characteristics using a drop tube furnace (DTF), a furnace with a ceramic tube length of 1200 mm, and an inner diameter of 72 mm. An electric heater is used to heat the furnace to around 1100 °C, indicated for the PC Boiler. The dried sample is fed into the furnace using a screw feeder with a flow rate of 50-100 gr/h. The premier air flow rate is 12.5 l/h, and the secondary air is 10 l/h. A probe with a diameter of 55 mm connected to a thermocouple is inserted into the furnace. The probe's position is adjusted to 600 °C to simulate the superheater area (slagging potential). After 1 hour, the probe was pulled out and cooled at room temperature, then observed, and ash deposits were taken from the DTF probe.

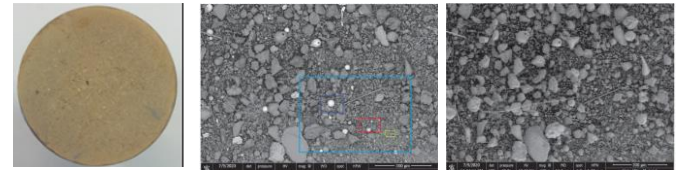
Scanning Electron Microscope (SEM) of model Quanta 650 of FEI was used with a backscattered, secondary electron and the Oxford Energy Dispersive Spectroscopy (EDS) detectors. The high vacuum environment and the low vacuum environment are also available, enabling the measurements of nonconducting samples without any coatings

2.3 Results

Our previous studies on coal combustion with 10% biomass sawdust found that the safe limit for the probe temperature was 600 C, indicating that 10% cofiring was safe for supercritical boilers. This investigation was carried out to strengthen this hypothesis by testing the supercritical 600 probes. This study attempts to observe more deeply by providing more details using a different tool, the Quanta 650. The initial observations yielded the following results.

Fig. 1(a) is an image of a probe that has been processed in DTF, Fig. 1(b) is a BSE (Back-Scattered Electron) with a light color that represents a high number of electrons, while Figure 1(c) represents SE (Secondary Electron). The dominant morphology and grain size could

indicate the severity of slagging, with a few high-electron elements that are under 100 microns in size. From the two figures, only a few elements are above 100 microns in size. It shows no melting in this 100x magnification view. Based on Bo Wei's method [12], the constituent elements of the particles (also the properties of each of these elements) will be used to predict and evaluate related slagging tendencies.



(a) (b) (c)

Fig. 1. Ash depositions

Fig. 2 is an enlargement of Fig. 1 (b), and this image will be the focus of attention, which is separated into many colored boxes. Aside from spectrums 1 to 9, the yellow box indicates site A, the green box represents site B, the red box represents site C, and the blue box represents site D. Further discussion will be explained later related to each box.

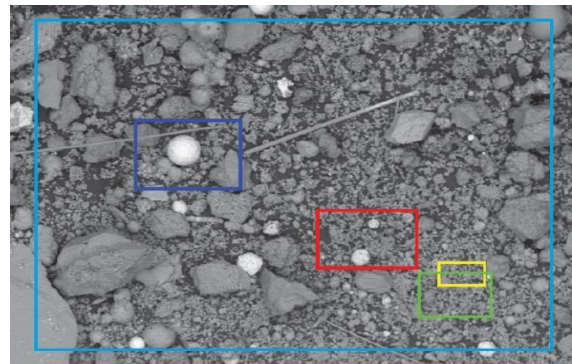


Fig. 2. Ash depositions

Fig. 3 is a spectrum sampling point that represents the material contained in the image. Based on the spectrum of the elements in each of which are dominant in a certain spectrum. In spectrum 1, the highest element is Ca 23.1%, followed by S 18% then O, Si, Al, Fe, Na, K, and Mg, In spectrum-2 the dominant Fe 50.4% O 33.4% C 6.4%, Si 4.5%, and low Al, Ca, S, Na, Mg. But Materials with patterns such as a spectrum of 2 microns are small in number. In spectrum 3 is similar to spectrum 2; it has high Fe 55.3%, O 33.2%, Si 4.6%, other materials such as Al, Cr, etc., with small amounts. Spectrum 4 is similar to spectrum 1, has O 47.9% Ca 19.9%, S17.2%, C 4.9%, other Al minor.

From the morphological observations and incorporation of the spectrum and the distribution of the similar elements from the picture, observations based on this spectrum indicating the addition of sawdust biomass is still within safe and reasonable limits based on the slagging fouling review. The following is a site-based review (area box consisting of A, B, C, and D).

Site A (Yellow box)

The morphology of the size is mostly under 10 microns. However, some appear to be combined. It is found between the sticky particles but shows no massive stickiness; there are still sticky hollow cavities showing that it is more fragile to shoot lower treatment and fall off easily. The constituent elements of the order O, Si, Al, Ca, and C indicate that the constituent sequences are harmless.

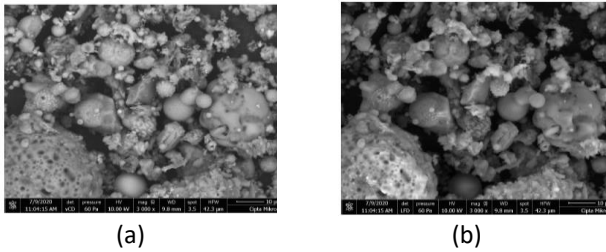


Fig. 3. 3000× magnification SEM images from the (a) Back-Scattered Electron and (b) Secondary Electron detectors

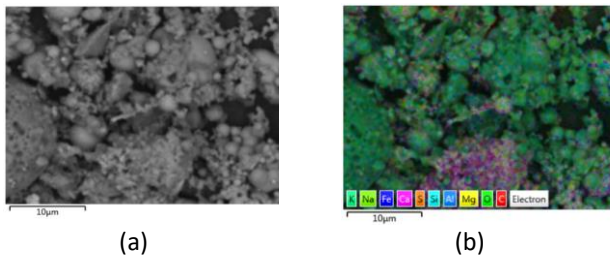


Fig. 4. Elemental distribution (b) based on the backscattering image of SEM (a). The area shown in Fig. (a) is slightly shifted from that of Fig. 3.

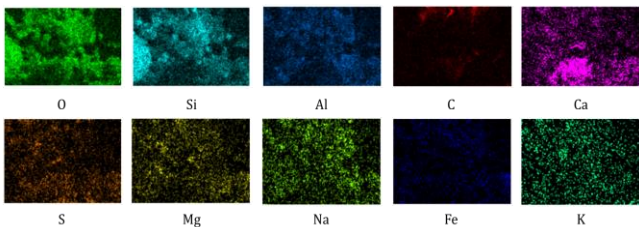


Fig. 5. Elemental mapping of O, Si, Al, C, Ca, S, Mg, Na, Fe, and K with the corresponding overlaid image shown in Fig 4(b)

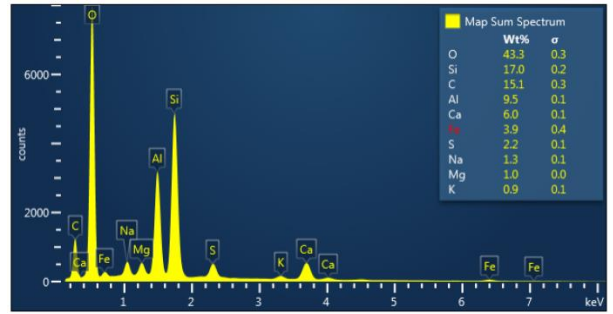


Fig. 6. The spectrum of site A corresponding to Fig. 4 (b)

Site B (Green box)

Area B is an area consisting of a green area that intersects with area A (Yellow). Generally similar to site A, namely O, Si, C, Al, Fe, and Ca. Balanced amounts of Fe and Ca are slightly different from site A, Fe Ca, although the size of the larger shape is the same as A, it does not appear sticky.

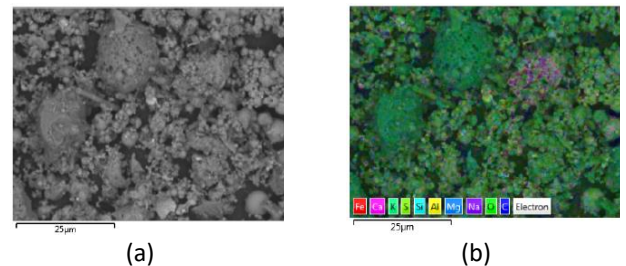


Fig. 7. Elemental distribution (b) based on the backscattering image of SEM (a)

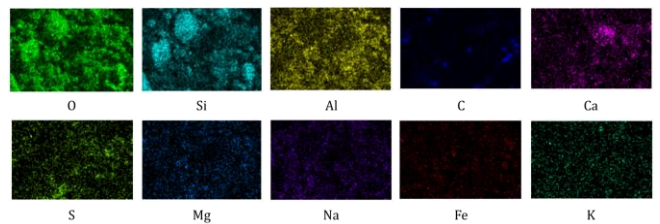


Fig. 8. Elemental mapping of O, Si, Al, C, Ca, S, Mg, Na, Fe, and K with the corresponding overlaid image shown in Fig6(b)

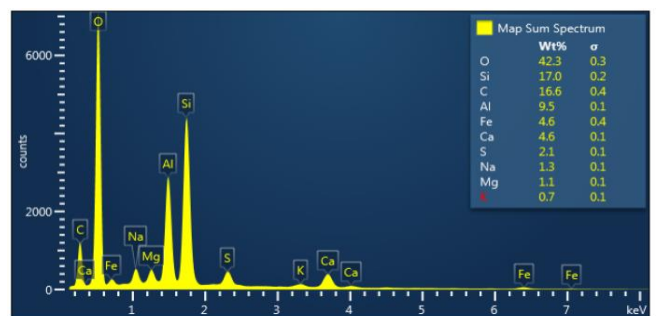


Fig. 9. The spectrum of site B corresponding to 7(b)

Site C (Red box)

In area C (red box), the magnification is performed at 300x. It looks worse in morphology but is still far below 75 microns, mostly below 25 microns. It clearly shows Fe balls are not as many main constituent elements, namely O, C, Si, Al, Ca, which are weak elements causing other minor slagging.

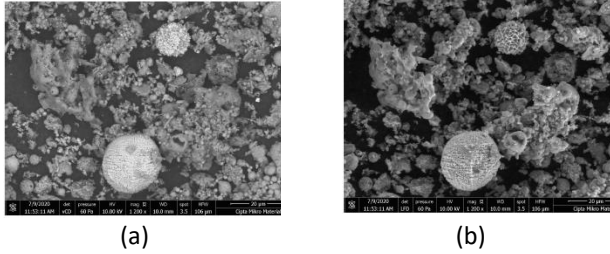


Fig. 10. 3000x magnification SEM images from the (a) Back-Scattered Electron and (b) Secondary Electron detectors

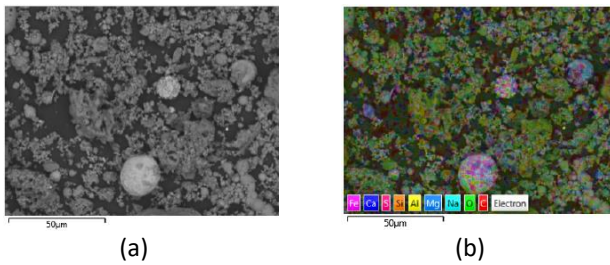


Fig. 11. Elemental distribution based on the backscattering image of SEM

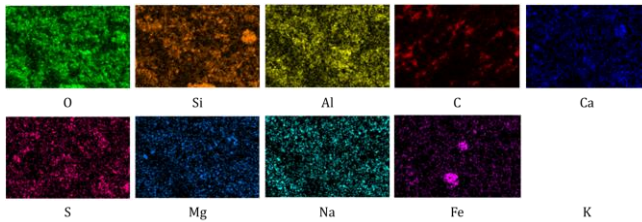


Fig. 22. Elemental mapping of O, Si, Al, C, Ca, S, Mg, Na, Fe, and K with the corresponding overlaid image shown in 11(b)

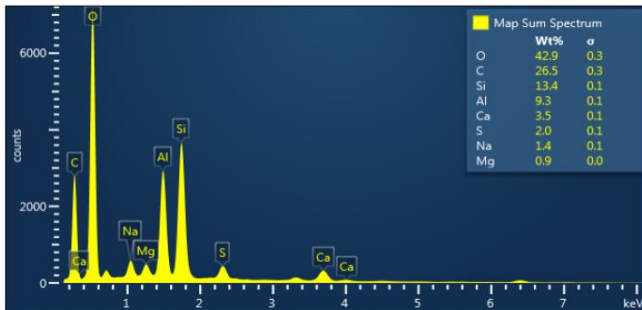


Fig. 33. The spectrum of site C corresponding to Fig. 11 (b)

Site D (Blue box)

It is a blue box area which is an area that contains balls with a size close to 50 microns. An Al rod has a length of more than 800 microns, approaching the area of the other red box, which is smaller than a sphere < 50 microns so that the microstructure is not dangerous, also no massive stickiness. As shown in Fig 17, FE content is quite high (10.4%), although it is still below O, C, Si.

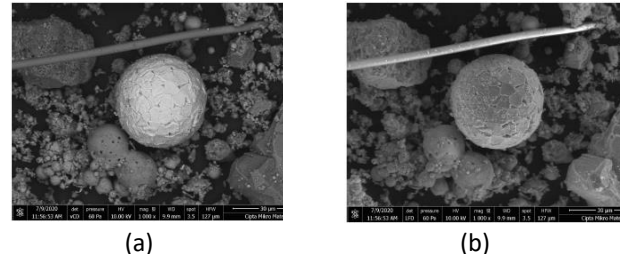


Fig. 44. 3000x magnification SEM images from the (a) Back-Scattered Electron and (b) Secondary Electron detectors

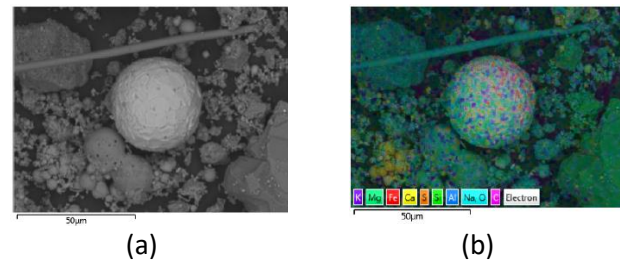


Fig. 55. Elemental distribution based on the backscattering image of SEM

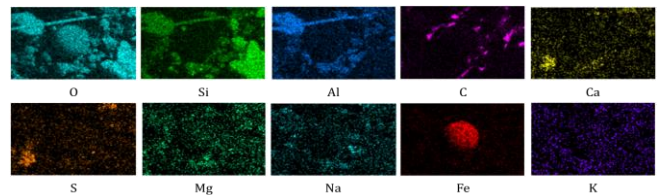


Fig. 66. Elemental mapping of O, Si, Al, C, Ca, S, Mg, Na, Fe, and K with the corresponding overlaid image shown in Fig. 55(b)

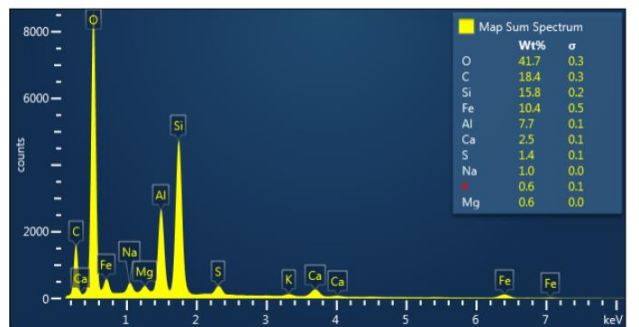


Fig. 77. The spectrum of site D corresponding to Fig. 55(b)

Based on the observations of the area boxes above and some comparisons, these SEM results show that they are more convincing than previous SEM observations. The use of 10% sawdust biomass in supercritical boilers is still within safe limits. Substituting 10% of biomass for coal could have a big impact on supercritical power plants in Indonesia, with a capacity of 5-6 GW

2.4 Conclusions

The slagging issue is still safe in follow-up observations from prior research involving the addition of 10% sawdust biomass to cofiring in PC Supercritical boilers using a combination of DTF and SEM methodologies. Further research is required on combustion in DTF at 700 C, where the maximum yield was attained in the previous treatment.

REFERENCE

- [1] Renewable Energy Agency I. Renewable Energy Prospects: Indonesia 2017.
- [2] Long H, Li X, Wang H, Jia J. Biomass resources and their bioenergy potential estimation: A review. *Renew Sustain Energy Rev* 2013;26:344–52. doi:10.1016/J.RSER.2013.05.035.
- [3] Szemmelveisz K, Szucs I, Palotás ÁB, Winkler L, Eddings EG. Examination of the combustion conditions of herbaceous biomass. *Fuel Process Technol* 2009;90:839–47. doi:10.1016/J.FUPROC.2009.03.001.
- [4] Yin C, Rosendahl LA, Kær SK. Grate-firing of biomass for heat and power production. *Prog Energy Combust Sci* 2008;34:725–54. doi:10.1016/J.PECS.2008.05.002.
- [5] Triyono B, Prawisudha P, Aziz M, Mardiyati, Pasek AD, Yoshikawa K. Utilization of mixed organic-plastic municipal solid waste as renewable solid fuel employing wet torrefaction. *Waste Manag* 2019;95:1–9. doi:10.1016/J.WASMAN.2019.05.055.
- [6] Darmawan A, Fitrianto AC, Aziz M, Tokimatsu K. Enhanced electricity production from rice straw. *Energy Procedia*, vol. 142, 2017. doi:10.1016/j.egypro.2017.12.043.
- [7] Liu Z, Zhang F, Liu H, Ba F, Yan S, Hu J. Pyrolysis/gasification of pine sawdust biomass briquettes under carbon dioxide atmosphere: Study on carbon dioxide reduction (utilization) and biochar briquettes physicochemical properties. *Bioresour Technol* 2018;249:983–91. doi:10.1016/J.BIORTECH.2017.11.012.
- [8] Fogarasi S, Cormos CC. Assessment of coal and sawdust co-firing power generation under oxy-combustion conditions with carbon capture and storage. *J Clean Prod* 2017;142:3527–35. doi:10.1016/J.JCLEPRO.2016.10.115.
- [9] Miyawaki N, Fukushima T, Mizuno T, Inoue M, Takisawa K. Effect of wood biomass components on self-heating. *Bioresour Bioprocess* 2021 81 2021;8:1–6. doi:10.1186/S40643-021-00373-7.
- [10] Zhang R, Lei K, Ye BQ, Cao J, Liu D. Effects of alkali and alkaline earth metal species on the combustion characteristics of single particles from pine sawdust and bituminous coal. *Bioresour Technol* 2018;268:278–85. doi:10.1016/J.BIORTECH.2018.07.145.
- [11] Zhou L, Jia Y, Nguyen TH, Adesina AA, Liu Z. Hydrolysis characteristics and kinetics of potassium-impregnated pine wood. *Fuel Process Technol* 2013;116:149–57. doi:10.1016/J.FUPROC.2013.05.005.
- [12] Wei B, Wu W, Liu K, Wang J, Chen L, Ma J, et al. Investigation of Slagging Characteristics on Middle and low temperature heat transfers by Burning High Sodium and Iron coal. <https://doi.org/10.1080/0010220220201830768> 2020. doi:10.1080/00102202.2020.1830768.